Acta Geodyn. Geomater., Vol. 21, No. 1 (213), 15–25, 2024
DOI: 10.13168/AGG.2024.0002

journal homepage: https://www.irsm.cas.cz/acta

ORIGINAL PAPER

COAL-ROCK COMBINED BODY FAILURE MECHANISM BASED ON CRACK DISTRIBUTION CHARACTERISTICS

Guangbo CHEN [1, 2], Jing ZHANG [1], Tan LI [1], Chuangye WANG [1], Wei TANG [1] and Eryu WANG [1] *

[1] *School of Mining and Coal, Inner Mongolia University of Science and Technology, Baotou, Inner Mongolia 014010, China*
[2] *College of Energy and Mining Engineering, Shandong University of Science and Technology, Qingdao 266590, China*

**Corresponding author's e-mail:* 2019956@imust.edu.cn

ARTICLE INFO

Article history:
Received 28 November 2023
Accepted 15 January 2024
Available online 24 January 2024

Keywords:
Coal-rock combined body
Rock component
Failure mechanism
Coal-rock interface
Energy transfer
Mechanical model

ABSTRACT

Many papers on axial compression tests of coal-rock combined bodies have observed the failure of rock components. However, the failure mechanism of the rock component has been the focus of debate among many scholars. One view is that the failure of the rock is due to the energy released during coal failure; the other view is that the failure of the rock is due to the inconsistent coal-rock lateral deformation resulting in tensile stress on the rock side of the coal-rock interface. In response to these two controversial failure mechanisms, coal-rock combined bodies with three coal-rock interface bonding methods (*AB* glue, direct contact, and graphite fluoride) were designed, and the axial compression tests were carried out. The results show that: (1) the damage cracks of the combined body are mainly distributed on the coal component, the stronger the interface adhesion, the easier it is to crack. (2) All three combined bodies showed rock component damage, and the number of cracks in the rock component was different at different interfaces of the combined bodies. The stronger the interfacial adhesion is, the easier it is to produce cracks, and the more the number of cracks in the rock component is. (3) The destruction of rock components is the result of energy transfer mechanism. Under the action of the test machine, the coal component is destroyed first, and a large amount of elastic energy is released instantaneously to the rock component, which reaches the energy storage limit of the rock and stimulates the destruction of the rock component. The tensile stress at the coal-rock interface plays a certain role in the propagation and penetration of cracks in the rock, but does not determine the damage of rock components. (4) The stronger the interfacial bonding, the greater the strength of the combined body. Based on the D-P criterion, the strength of coal rock at the interface of coal-rock combined body was analyzed. The strength of the coal body at the interface increases to a certain extent, and the strength of the rock mass at the interface decreases to a certain extent. (5) The stress distribution model of coal-rock combined body was constructed, and the internal mechanism of coal-rock component failure was further clarified. The coal and rock mass at the interface are the weak areas of the combined body, and the stress concentration in this area is the largest and the possibility of damage is the largest.

1. INTRODUCTION

In recent years, with the continuous progress and development of society, the demand for coal resources has become more urgent. The shallow coal resources have been exhausted, and the coal resources have gradually entered the deep mining stage (Chen et al., 2023). With the deepening of coal mining depth and the increase of mining range, the frequency and intensity of underground coal-rock geodynamic disasters are gradually increasing. The essence of underground dynamic disaster in coal mine is the sudden deformation and failure of coal rock, especially the rock burst (Feng et al., 2019; Cheng et al., 2016; Yu et al., 2013). The research on underground rock burst in coal mine is mostly focused on experiments, but the study of mechanical properties and instability mechanism of coal-rock system by coal-rock combined method is more in line with the actual situation in the field, and has become the focus of experts and scholars (Chen et al., 2020; Zuo et al., 2011; Zhang et al., 2020; Si et al., 2024). The instability failure mechanism of coal-rock combined body is of great significance to the study of instability failure of underground coal-rock system in coal mine.

Many experts have studied the failure mechanism of coal-rock combined body through mechanical tests (Chen et al., 2023; Zhang et al., 2023; Yang et al., 2022). Chai et al. (2023) performed uniaxial static-cyclic loading tests on a series of combined bodies with different roof lithologies, and investigated the damage and failure process of combined bodies under mining-induced stress conditions, particularly the mechanical response and damage evolution of coal and rock under cyclic disturbance. Bai et al. (2021) conducted uniaxial cyclic dynamic loading experiments with four different coal height ratios of combined bodies, analyzed the mechanical properties, failure modes,

Cite this article as: Chen G, Zhang J, Li T, Wang C, Tang W, Wang E: Coal-rock combined body failure mechanism based on crack distribution characteristics. Acta Geodyn. Geomater., 21, No. 1 (213), 15–25, 2024. DOI: 10.13168/AGG.2024.0002

and wave velocity evolution of combined bodies, discussed the process of rock burst under coupled static and dynamic loads in rock-coal-rock combined body. Zuo et al. (2018) conducted the uniaxial compression test on the coal-rock combined specimen of Qianjiaying coal and found the phenomenon of joint failure of coal and rock, which was mainly due to the rock failure caused by the elastic property released by the coal body at the time of failure. Gong et al. (2017) carried out uniaxial compression tests on coal-rock combined bodies with low loading rates under four different orders of magnitude, and found that with the increase of loading magnitude, the sample changed from the failure of coal to the joint failure of coal and sandstone. It is considered that the storage energy of the micro-unit before coal failure increases at a higher loading rate, gradually reaching a higher value, and at the same time releasing a larger energy. At this time, the bearing failure structure is the whole coal rock, resulting in joint failure of coal rock. Wang et al. (2013) carried out the uniaxial compression test on the coal-rock combined body of "roof-coal seam-floor" type, and found the phenomenon of common failure of coal and rock, and the rock failure mainly has two failure modes: shear failure and tensile failure. Chen et al. (2021) and Chen et al. (2022) found that the macroscopic failure of coal components is earlier than that of rock components through the uniaxial compression test of coal-rock combined body. At the same time, the energy transfer mechanism of coal-rock combined body is established, and it is considered that the failure of rock components is that the energy released after the failure of coal components is transferred to rock, and the failure of rock occurs from the beginning of primary cracks and fractures. Yang et al. (2020a) studied the mutual feedback mechanism of the failure process of coal-rock combined body, and considered that when the strong stress chain at the interface between the coal crack and coal-rock interface is greater than the rock strength, the coal crack develops rapidly into the rock and induces the rock failure, and the energy released by the rock failure aggravates the coal failure. Yang et al. (2020b) and Yang et al. (2019) carried out loading tests on combined coal and rock with different strength ratios, and found that the strength of coal determined the main body of failure. When the strength of rock reached 4 times that of coal, the rock was no longer destroyed. The dissipative, frictional and kinetic energy evolution of coal and rock were related to whether their failure occurred or not, and the energy driving mechanism of coal-rock combined body failure was discussed.

The above experts believe that the failure of rock in coal-rock combined body is the result of the release of failure energy of coal components, but many experts hold different views on this. Gao et al. (2020) used a high-speed camera to observe that rock failure occurred before the coal failure, and through the numerical simulation study, it was found that the tensile failure of the rock was caused by the tensile stress on the rock side of the coal-rock interface caused by the inconsistency of the coal-rock lateral deformation, rather than by the energy released by the coal failure. Shen et al. (2021) believed that the failure of rock components in the coal-rock combined body is mainly related to the expansion effect of the coal-rock interface. Zhang et al. (2012) conducted uniaxial compression and triaxial compression test on three kinds of coal-rock combined body, and found that tensile failure occurred in the coal body part of the coal-rock combined body, and a few penetrating tensile cracks occurred in the rock part, which was mainly due to the first failure of the coal part of the combined body, resulting in local stress concentration in the rock part, which leads to tensile cracks in the rock part while the coal body part is further broken.

The failure mechanism of rock components in coal-rock combined body has always been the focus of academic debates. At present, there are two views on the failure mechanism of rock components, one view is that the failure of rocks is caused by the energy released during coal failure; the other view is that the failure of rocks is caused by the tensile stress on the rock side of the coal-rock interface caused by the inconsistency of coal-rock lateral deformation. In response to these two controversial failure mechanisms, the axial compression tests were carried out on the combined body of three different coal-rock components from the coal-rock interface, and the failure mechanism of rock components in the coal-rock combined body was discussed. It provides a reference for further elucidating the failure mechanism of rock components in coal-rock combined body and the energy evolution mechanism of coal-rock components. At the same time, it also has certain reference value for elucidating the instability failure mechanism of coal-rock system and the prevention and control of rock burst disasters.

2. VERIFICATION TEST OF ROCK COMPONENT FAILURE MECHANISM OF COAL-ROCK COMBINED BODY

The axial loading test was carried out on the coal-rock combined body. At the initial stage of loading, the coal-rock components were not damaged, and there was no friction at the coal-rock interface. With the continuous loading, the coal-rock components were deformed radially, and friction was generated at the coal-rock interface. Due to the different transversal deformability of coal-rock components, the lateral strain of coal-rock components is different. Many experts believe that the failure of the rock components of the combined body is caused by the inconsistent radial deformation of coal and rock at the coal-rock interface, and the friction generated at the coal-rock interface leads to tensile stresses in the rock components near the interface, resulting in tensile failure. If the friction force at the coal-rock interface is effectively eliminated or greatly reduced, the rock component still has tensile failure, then it is proved that the failure of the rock component

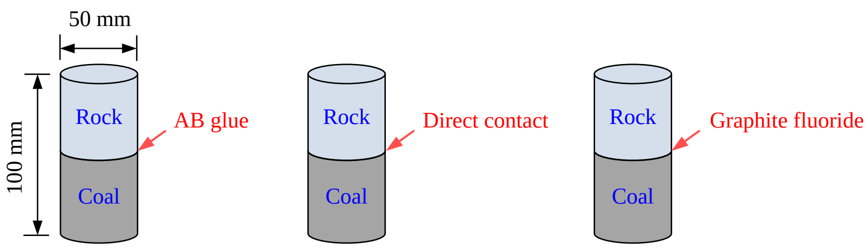

Fig. 1 Combined body model of different contact modes of coal-rock interface.

is not related to the inconsistency of radial deformation of coal rock. Based on the above point of view, starting from the friction force of coal-rock interface, three kinds of interface contact modes of coal-rock components are designed:

(1) The coal-rock components are bonded with AB glue, and the adhesion is good. During the loading process of the combined body, the friction force at the coal-rock interface is large. The combined body is referred to as YM-1 combined body.

(2) The coal-rock components are in direct contact with each other without any material, and the coal-rock interface has a certain friction force during the loading process of the combined body, which is referred to as the YM-2 combined body. The friction force at the coal-rock interface of the YM-2 combined body is smaller than that of the YM-1 combined body.

(3) Graphite fluoride is smeared between coal and rock components (it should be noted that graphite fluoride is a solid lubricant with good wear resistance and pressure resistance, and still has good lubrication properties under high temperature, high speed and high pressure). In the process of loading, the coal-rock interface is relatively smooth and the friction is small. The combined body is referred to as the YM-3 combined body.

According to the above reasoning, if the failure of rock components occurs in the YM-3 combined body, it can be proved that the failure of rock components is not caused by the inconsistent radial deformation of coal and rock at the coal-rock interface; if the YM-1, YM-2 and YM-3 combined bodies all have the failure of rock components, it shows that the failure of rock components is caused by the energy released by the failure of coal components to rock components. According to the above ideas, we have carried out the verification test of rock component failure mechanism of coal-rock combined body.

The coarse sandstone and coal required for the test were taken from Xing 'an Coal Mine in Hegang City, Heilongjiang Province, and transported back to the laboratory after drilling, cutting, grinding and other processes to produce standard combined specimens with a coal-rock ratio of 1:1 (diameter 50 mm, height 100 mm). After processing, the specimens with obvious fractures and cracks on the surface and those whose dimensions and evenness are not up to the requirements can be removed. The coal-rock sequence is above the rock and under the coal. The coal-rock model is shown in Figure 1. In order to ensure the reliability of the test results and the scientific nature of the test, five combined specimens were prepared and five parallel tests were carried out. In order to study the distribution of cracks and fractures in the combined body under loading, 1~2 layers of cling film were wrapped outside the combined body to avoid the peeling fragments falling on the test bench during loading, and a layer of sulfuric acid paper was wrapped outside the cling film, and the crack distribution could be depicted on the sulfuric acid paper after the specimen was damaged.

The uniaxial compression test of coal-rock combined body is carried out by using TAW-2000kN microcomputer-controlled electro-hydraulic servo rock testing machine (Fig. 2). The loading mode is displacement loading and the loading rate is 0.005 mm/s. In the axial compression test, when the strain rate (loading rate) of the specimen is less than 10^{-4}/s, the effect of loading rate on the compressive strength of coal specimen is negligible and can be ignored. This loading mode can be regarded as static loading.

3. STRENGTH ANALYSIS OF COAL-ROCK COMBINED BODY

Figure 3 shows the compressive strength test values and average values of the three combined bodies. The average compressive strength of YM-1 combined body with AB glue interface is 16.80 MPa, the average compressive strength of YM-2 combined body with direct contact is 15.54 MPa, and the average compressive strength of YM-3 combined body at graphite fluoride interface is 14.54 MPa. The compressive strength of YM-1 combined body is the largest, and the compressive strength of YM-3 combined body is the smallest. The greater the interface friction, the greater the strength of the combined body; the smaller the interface friction, the smaller the strength of the combined body. The difference in the strength of the combined body is related to the interface effect. The interface effect has a certain influence on the strength of the enhanced combined body. The difference in strength between the three combined bodies is small, so the interface effect is not the main controlling factor for the strength

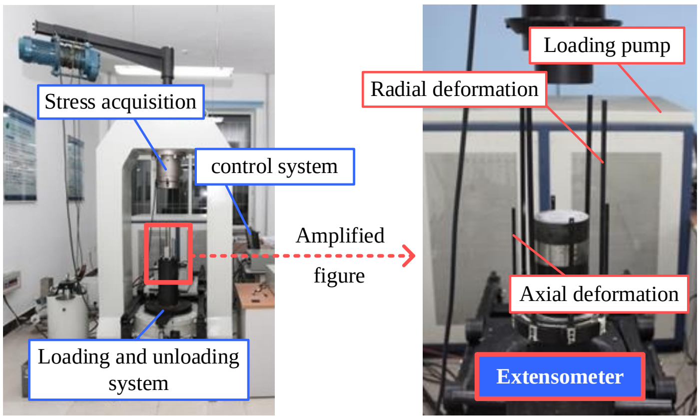

Fig. 2 The test system.

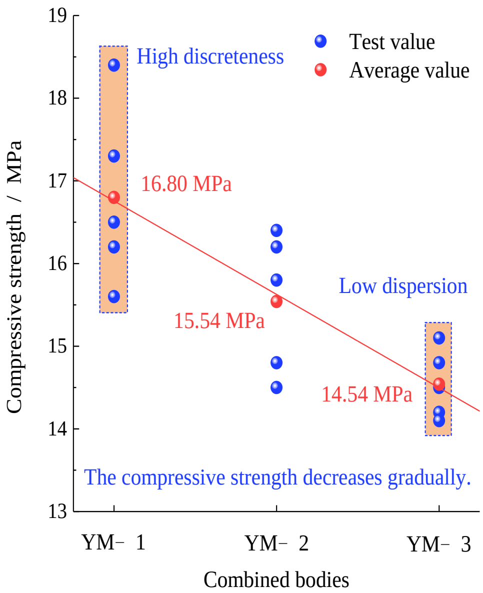

Fig. 3 Strength of coal-rock combined body.

of the combined body. On the other hand, it can also be seen that the strength test data of YM-1 combined body with AB glue interface is more discrete, and the strength test data of YM-3 combined body with graphite fluoride interface is less discrete.

It is worth noting that the interface effect of coal-rock combined body has a certain influence on its strength, but has no effect on the failure mechanism of coal-rock. It can be inferred that in the coal-rock combined body test, according to the formation of coal-rock strata, the strength of the combined body bonded with AB glue is more in line with the actual coal-rock strength of the project, and the strength measured by the laboratory of the combined body with direct contact between coal and rock is lower than that of the engineering practice.

4. DISCUSSION ON CRACK DISTRIBUTION CHARACTERISTICS AND FAILURE MECHANISM OF COAL-ROCK COMBINED BODY

4.1. CRACK DISTRIBUTION CHARACTERISTICS OF COAL-ROCK COMBINED BODY

According to the test scheme, the uniaxial compression tests are carried out on three coal-rock combined bodies, and the distribution of cracks after damage of the combined bodies is shown in Figure 4. The black cracks indicate the cracks existing in the coal component, the blue cracks indicate the cracks existing in the rock component or the cracks coexisting with the coal rock component, and the red cracks indicate the main control cracks of coal rock damage. It is necessary to explain that there are many tiny cracks in addition to the cracks listed above. The length and width of these cracks are small, which have no effect on the failure analysis of the specimen and are not marked in Figure 4.

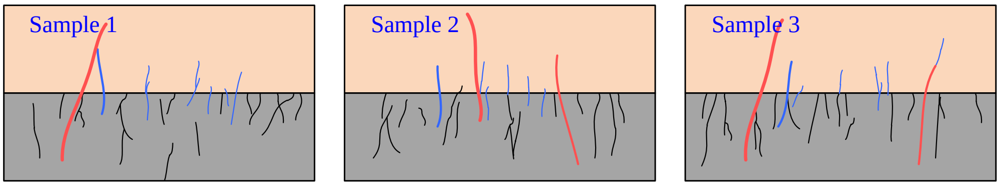

(a) YM-1 combined body

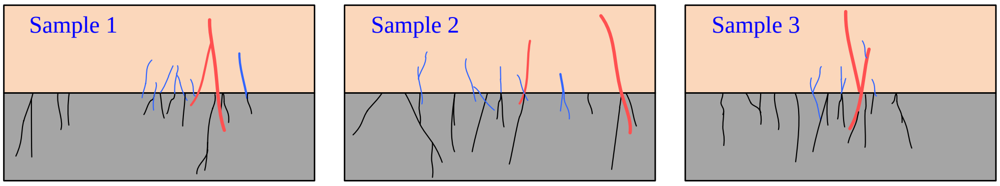

(b) YM-2 combined body

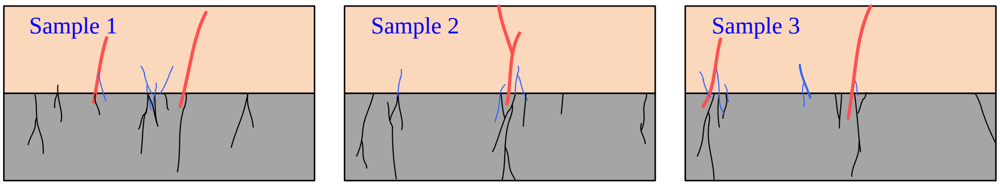

(c) YM-3 combined body

Fig. 4 Crack distribution characteristics of combined bodies with different interface contact modes.

It can be seen from Figure 4:

(1) From the point of view of crack distribution position, the cracks of YM-1 combined body are mostly distributed near the coal-rock interface and mainly concentrated on the coal components; the cracks in the YM-2 combined body are also mainly distributed near the coal-rock interface and mostly concentrated in the coal components, and the cracks have a downward extension trend, and even some cracks penetrate the coal components; the cracks of the YM-3 combined body are mainly distributed in the coal components, showing an obvious deepening trend, and there are 1-2 cracks running through the coal components. This is mainly related to the interface effect of coal-rock combined body.

(2) From the number of cracks, the number of cracks in the YM-1 combined body is 26, 23 and 27, the number of cracks in the YM-2 combined body is 21, 23 and 22, the number of cracks in the YM-3 combined body is 19, 19 and 18, the number of cracks after failure in the YM-1 combined body is more, and the number of cracks after failure in the YM-3 combined body is less. From this point of view, the combined body of binder interface is more likely to produce cracks, and the combined body of graphite fluoride interface produces fewer cracks. The reason is that it is mainly related to the adhesion of the adhesive, which has a large friction force at the component interface and produces a certain tensile stress at the time of destruction.

(3) From the point of view of the failure state of rock components, there is a failure of rock components after the failure of the combined body of YM-1, YM-2 and YM-3, and there are cracks in the interface area of cracks in rock components and cracks in coal components. The cracks in rock components are mainly concentrated near the coal-rock interface. In addition, it is found that the rock component of the YM-1 combined body has more cracks, followed by the YM-2 combined body, and the YM-3 combined body has the least. From this, no matter what kind of interface contact mode, the rock components of the combined body are damaged under uniaxial compression conditions, and there are more cracks in the rock components of the combined body with binder interface and less cracks of the combined body at the fluoride graphite interface.

(4) From the perspective of crack development and penetration of rock components, although cracks appear in the rock components during the loading process of the three combined bodies, the development and penetration of cracks are quite different. The cracks in the rock component of the YM-1 combined body penetrate more into the coal component and basically penetrate the coal component, forming a larger crack in the coal rock component, and the crack length is longer; the cracks in the rock component of the YM-2 combined body also develop into the coal component, but only about 1/2 of the coal component, and the crack length is shorter than that of the YM-1 combined body; The cracks in the rock component of the YM-3 combined body basically exist in the rock component, and although they develop and penetrate into the coal component, but only about 1/4. The root cause of the above phenomenon is the adhesion of the binder on the coal-rock interface. The destruction of the rock component leads to the radial deformation of the rock component,

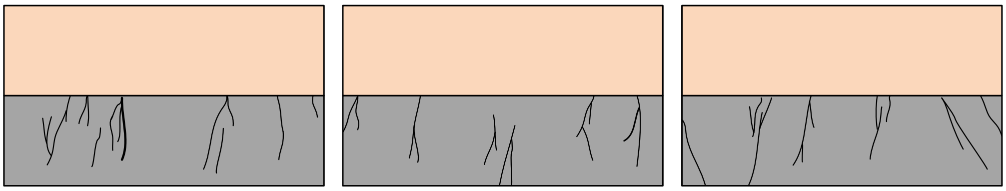

Fig. 5 Other failure forms of combined bodies.

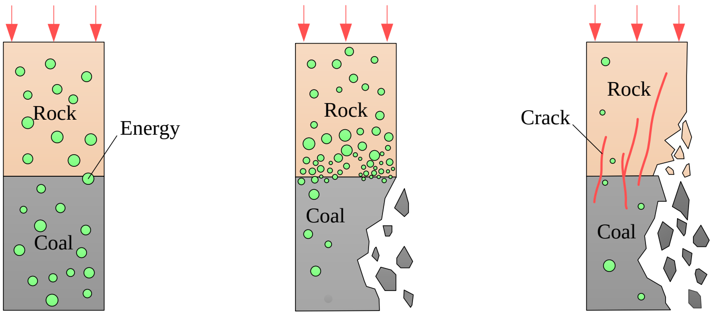

Fig. 6 The energy transfer mechanism in the failure process of coal-rock combined body.

and the friction at the interface leads to the tension in the coal component near the interface, resulting in cracks in the coal component. The stronger the interface adhesion, the more penetrating the coal-rock cracks.

In addition to the failure pattern in Figure 4, the failure pattern in Figure 5 also appears in the test, that is, the rock component in the coal-rock combined body is not destroyed, and only the coal component is destroyed, and this situation occurs in all three combined bodies. As can be seen from Figure 5, the crack length in the coal component is larger, even running through the whole coal body, and the crack is more dispersed, not only concentrated near the interface, but also in the middle and lower part of the coal component.

4.2. DISCUSSION ON FAILURE MECHANISM OF COAL-ROCK COMBINED BODY BASED ON CRACK DISTRIBUTION CHARACTERISTICS

Starting from the failure characteristics of coal-rock combined body, the analysis of the instability failure mechanism of coal-rock combined body can better reflect the actual engineering situation. From the failure patterns of the three combined bodies, the joint failure of coal and rock occurs under the uniaxial compression conditions of all three combined bodies, and it is found during the test that the destruction of coal is earlier than that of rock, which is consistent with the results of the literature (Yang et al., 2019; Yang et al., 2020). The rock is destroyed under the three kinds of coal-rock interface bonding modes, which indicates that the destruction of rock components is not related to the bonding mode of coal-rock interface, and it is not the friction of coal-rock interface that leads to the tensile stress of rock interface. Based on this, it can be inferred that the failure of rock components is caused by the transfer of energy released by coal components to rock components, and occurs under the excitation of energy released by coal components. However, the failure of rock components is not entirely the result of the failure energy transfer of coal components. In addition to the main controlling factors excited by energy, the adhesion of coal-rock interface has a certain influence on the crack propagation after the failure of rock components. This conclusion can be seen from the development and penetration of rock cracks on the coal-rock interface. The combined body with good coal-rock interface bonding has good rock component crack penetration, while the combined body with poor interface adhesion has poor rock component crack penetration. The development and penetration of the crack is mainly related to the tensile stress at the crack tip, so the combined body with good adhesion is easy to penetrate because of the larger tensile stress of the coal-rock crack. On the other hand, there is another kind of failure phenomenon in the three combined bodies, that is, the coal component is destroyed and the rock component is not destroyed. This is because although the energy released during the failure of the coal component is transferred to the rock, it does not reach the energy storage limit of the rock component, so the rock component will not be destroyed.

Based on the above analysis, the energy evolution model of coal-rock combined body is constructed, as shown in Figure 6. The failure mechanism of the coal-rock combined body under the

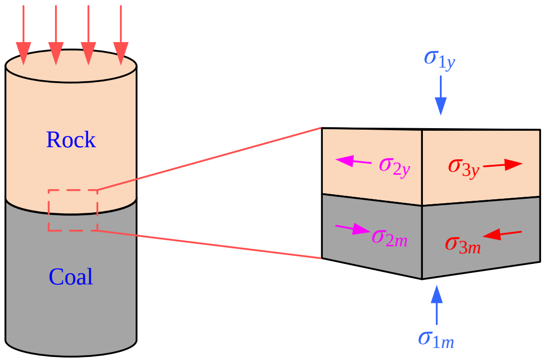

Fig. 7 Force analysis of microelement at the interface of coal-rock combined body.

load condition is as follows: the coal-rock combined body continuously accumulates energy under the action of the test machine, and there is energy dissipation and energy accumulation in the process. The energy dissipation is greater than the energy accumulation, and the combined body is in a state of continuous energy accumulation, as shown in Figure 6(a). When the energy accumulates to a certain extent and reaches the energy storage limit of the coal component, the coal component is destroyed, and a large amount of elastic energy is released instantaneously to transfer to the rock component, and a large amount of elastic energy is accumulated at the coal-rock interface, as shown in Figure 6(b). When the accumulated elastic energy reaches the energy storage limit of rock, it will lead to the destruction of rock components, cracks, fractures and the collapse of rock blocks, as shown in Figure 6(c). If the energy storage limit of the rock component is not reached, the rock component will not be destroyed, such as the failure state shown in Figure 5 in this experiment. This is the instability failure mechanism of coal-rock combined body under loading conditions.

5. DISCUSSION OF COAL-ROCK INTERFACE STRENGTH THEORY

In order to analyze the strength of coal-rock combined body, it is assumed that the relative displacement has not occurred at the interface of coal-rock combined body. Let the elastic modulus of rock components be E_y, the elastic modulus of coal components be E_m, $E_y > E_m$, the Poisson's ratio of rock components be μ_y, the Poisson 's ratio of coal components be μ_m, $\mu_m > \mu_y$. Due to the different Poisson's ratio of coal and rock components, the shear force will be generated at the coal-rock interface, and the shear force in the coal component and the shear force in the rock component is the relationship of action and reaction force. The shear force in the coal component points to the center, which has a certain binding effect on the expansion of the coal component, while the shear force of the rock component is far away from the center. In a certain range near the coal-rock interface, the coal component is divided into three-dimensional stress state. The micro-element force analysis at the coal-rock interface is shown in Figure 7.

From the deformation continuity condition and the static equilibrium relationship, it can be obtained that

$$\sigma_{iy} = \sigma_{im} = \frac{E_y \cdot \mu_m - E_m \cdot \mu_y}{E_y(1+\mu_m) - E_m(1+\mu_y)} \cdot \sigma_1 \tag{1}$$

The formula $i = 2, 3$; $\sigma_1 = \sigma_{1y} = \sigma_{1m}$

It can be seen that $\sigma_{2y} = \sigma_{2m} = \sigma_{3y} = \sigma_{3m}$.

Druker-Prager criterion (D-P criterion for short) is a criterion reflecting the strength of geotechnical materials. D-P criterion not only takes into account the effect of intermediate principal stresses, but also the effect of hydrostatic pressure, which overcomes the main weakness of the M-C criterion and has been widely used in the numerical calculation and analysis of geotechnical mechanics and engineering in China. According to the D-P criterion, the strength of elastic-plastic material can be expressed by Formula (2).

$$I_1 = \sigma_{ii} = \sigma_1 + \sigma_2 + \sigma_3 \tag{2}$$

In the formula, $I_1 = \sigma_{ii} = \sigma_1 + \sigma_2 + \sigma_3$ is the first invariant of stress; $J_2 = \frac{1}{2} S_i S_i = \frac{1}{6}[(\sigma_1 - \sigma_2)^2 + (\sigma_2 - \sigma_3)^2 + (\sigma_3 - \sigma_1)^2]$ is the second invariant of stress deviation; α, K are experimental constants related to the internal friction angle φ and cohesion c of rock $\alpha = \frac{2\sin\varphi}{\sqrt{3}(3-\sin\varphi)}$, $K = \frac{6c\cos\varphi}{\sqrt{3}(3-\sin\varphi)}$.

When $\sigma_2 = \sigma_3$, Formula (2) can be simplified to

$$\sigma_1 = \frac{\sigma_3(3 - 5\sin\varphi) + 6c\cos\varphi}{3 + \sin\varphi} \tag{3}$$

Assuming that $\sigma_2 = \sigma_3 = 0$ far from the coal-rock interface, the coal-rock strength σ_{yl} is

$$\sigma_{yl} = \frac{6c\cos\varphi}{3 + \sin\varphi} \tag{4}$$

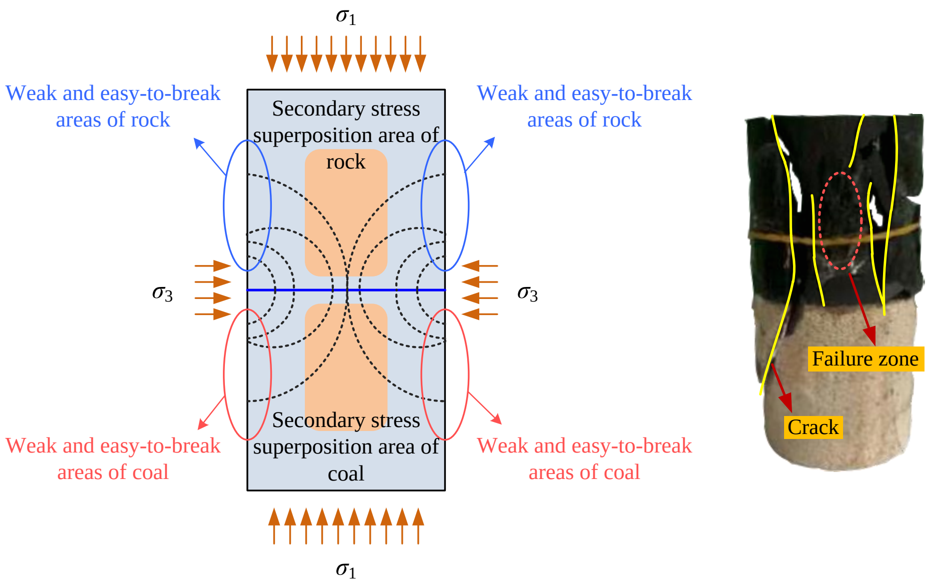

Fig. 8 Stress distribution of coal and rock.

The strength of coal at the coal-rock interface is obtained by combining Formula (3) and Formula (1):

$$\sigma_m = \frac{\sigma_{yl}}{1-\alpha\cdot\lambda} \tag{5}$$

In the formula,
$\alpha = \frac{3-5\sin\varphi}{3+\sin\varphi}$, $\lambda = \frac{E_y\cdot\mu_m - E_m\cdot\mu_y}{E_y(1+\mu_m)-E_m(1+\mu_y)}$, $0<\alpha<1$, $0<\lambda<1$, therefore, $0<\alpha\cdot\lambda<1$.

It can be seen from Formula (5) that the strength of the coal component at the coal-rock interface is greater than that of the coal component away from the interface, which means that the existence of the coal-rock interface plays a certain role in strengthening the strength of the coal body at the interface. Similarly, the strength of the rock component at the coal-rock interface is less than that of the rock component away from the interface. The existence of the coal-rock interface has a certain weakening effect on the strength of the rock mass at the interface.

The above analysis of the influence of the interface effect on the strength of coal and rock near the interface, the strength of coal and rock materials is closely related to its own ultimate energy storage, the greater the strength, the more the ultimate energy storage; the smaller the strength, the less the ultimate energy storage. From the above analysis, it can be seen that the strength of rock components at the coal-rock interface is weakened, so the ultimate energy storage of rock components at the coal-rock interface is reduced, and when the energy released by the destruction of coal components is transferred to the rock components at the coal-rock interface, the rock components near the interface are more prone to crack and damage.

6. DISCUSSION ON FAILURE MECHANISM OF COAL-ROCK SYSTEM IN ENGINEERING ANGLE

Due to the large difference in mechanical properties of sandstone and coal rock itself, the coal-rock combined system will produce different deformation when loaded. Under the same load, the axial strain and circumferential strain of the sandstone part at both ends of the combined body are smaller than the axial strain and circumferential strain of the coal part. This is the indirect cause of the destruction of the rock component. With the continuous loading of the testing machine, more energy is accumulated in the coal component. When the energy storage limit of the coal body is reached, the coal body is destroyed, and the energy released during the failure is transmitted to the rock component through the coal-rock interface, and the energy storage limit of the rock component is reached leading to the destruction of the rock component. This is the direct cause of rock component destruction. The compressive mechanical model of the combined specimen is shown in Figure 8. It can be seen from the figure that the coal and rock mass at the coal-rock interface are the weak areas of the combined body, which are easy to be destroyed under load conditions. The accumulation of energy is closely related to stress concentration. At the upper and lower edges of the coal-rock interface (coal extrusion fragile zone), the stress concentration degree is the largest, and the possibility of failure is the largest (Yu et al., 2020), followed by the secondary stress superposition zone of coal and rock mass. When the vertical stress increases, the stress superposition gradually increases until failure, forming a penetrating crack from coal to rock mass. The crack distribution pattern of the sample in Figure 4 and the failure physical diagram of the sample in Figure 8 illustrate this rule well.

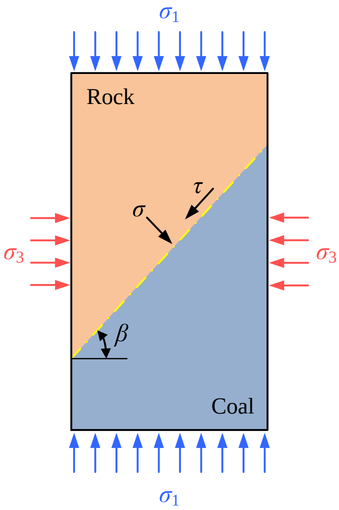

(a) The dip angle of coal-rock interface is β.

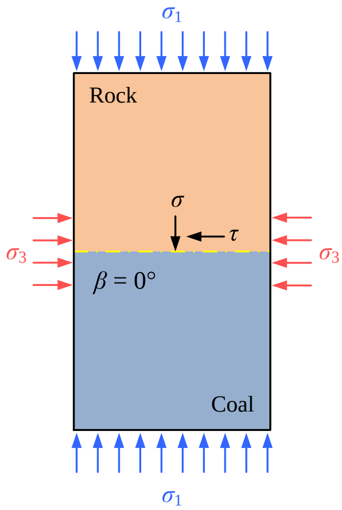

(b) The dip angle of coal-rock interface is 0°.

Fig. 9 Mechanical model of combined body under compression.

In this paper, compression experiments were carried out for the coal-rock interface dip angle 0° combined body, and the case where the coal-rock interface dip angle is not 0° is added here as a discussion. Many researchers have found that when a certain angle exists at the coal-rock interface, the damage range gradually increases with the gradual increase of the interface dip angle. It is assumed that: (1) the strength of coal-rock combined body obeys Mohr-Coulomb criterion; (2) the structural plane of inclined coal-rock mass obeys Mohr-Coulomb criterion; (3) the coal-rock combined body with dip angle is homogeneous.

As shown in Figure 9, according to Mohr stress circle theory, the normal stress σ and shear stress τ of the contact surface of coal-rock combined body with dip angle can be calculated by the first and third principal stresses:

$$\begin{cases} \sigma = \frac{1}{2}(\sigma_1+\sigma_3)+\frac{1}{2}(\sigma_1-\sigma_3)\cos(2\beta) \\ \tau = \frac{1}{2}(\sigma_1-\sigma_3)\sin(2\beta) \end{cases} \tag{6}$$

In the formula,

σ_1– The maximum principal stress of coal-rock combined body is axial stress;

σ_3– The minimum principal stress is the confining pressure stress;

β– The angle between the coal-rock interface and the horizontal plane, σ and τ will increase with the increase of dip angle β.

Assuming that the shear strength of the structural plane between the coal-rock combined bodies obeys the Coulomb criterion, then

$$\tau = c + \sigma \tan\varphi \tag{7}$$

In the formula, c=c_0, c_w; φ=φ_0, φ_w;

Where,

c_0– Cohesion of coal-rock combined system, MPa;

c_w– Cohesion of coal-rock structural plane, MPa;

φ_0– Internal friction angle of coal-rock combined system, °;

φ_w– Internal friction angle of coal-rock structural plane, °.

Combining (6) with (7), we can get:

$$\sigma_1 = \sigma_3 + \frac{2(c_w+\sigma_3\tan\varphi_w)}{(1-\tan\varphi_w\cot\beta)\sin(2\beta)} \tag{8}$$

The Formula (8) is the failure strength condition of the structural plane of the coal-rock combined body. Due to the use of coal and rock in this experiment, the cohesion and friction angle in this paper is only to follow the traditional concept, which is used to describe the overall nature of coal and rock mass. This nature is more manifested in the nature of the contact surface between coal and rock mass. In formula (8), φ_w is the internal friction angle of the coal-rock structural plane, which can be obtained according to the Mohr circle and the envelope line, and β is the angle between the coal-rock structural plane and the horizontal plane. The derived formula is only used for the coal-rock combined body with dip angle, and the condition of shear slip failure on the coal-rock contact surface under confining pressure. It can be seen from Formula (8) that the internal friction angle φ_w of the coal-rock structural plane coated with graphite fluoride is smaller, and the internal friction angle φ_w of the coal-rock structural plane bonded by AB glue is larger, so the coal-rock interface coated with graphite fluoride is more likely to be destroyed than the other two interfaces.

7. CONCLUSION

Many papers on axial compression tests of coal-rock combined bodies have observed the phenomenon of rock component failure. However, the failure mechanism of the rock component has been the focus of debate among many scholars. From the point of view of coal-rock interface bonding and based on the distribution characteristics of coal-rock failure cracks, the failure mechanism of rock components of coal-rock combined body is discussed, and the following understandings are obtained:

(1) Under the condition of uniaxial compression, the rock components of the combined body of the three coal-rock interfaces contact modes are destroyed, and the failure cracks are mainly distributed near the coal-rock interface and mainly concentrated on the coal components. The stronger the bonding effect of coal-rock interface, the easier it is to produce cracks, and the more the number of cracks in rock components.

(2) The failure mechanism of rock components in coal-rock combined body is analyzed. The destruction of rock components is the result of the interaction of two mechanisms, and the energy released by the destruction of coal components is transferred to the rock components to induce the destruction of rock components, which is the dominant mechanism of rock component destruction. This mechanism determines whether the rock components are destroyed or not, while the tensile stress caused by friction and adhesion at the coal-rock interface can promote the expansion and penetration of rock component cracks and increase the damage degree of rock components. This mechanism promotes the damage of rock components, not the dominant mechanism.

(3) The influence of interface effect on the strength of coal-rock combined body is analyzed theoretically. The stronger the bonding of the coal-rock interface, the greater the compressive strength of the combined body. Affected by the interface effect, the strength of the rock component at the coal-rock interface is “weakened”, which reduces the energy storage limit of the rock component at the interface. When the energy released by the failure of the coal component is transferred to the rock component at the interface, rock components are more prone to crack and failure.

(4) The stress distribution model of coal-rock combined body is constructed, and the internal mechanism of coal-rock component failure is further clarified. The coal and rock mass at the coal-rock interface is the weak area of the combined body. Where the degree of stress concentration is the highest and the possibility of failure is the greatest, followed by the secondary stress superposition area of coal and rock mass, when the vertical stress increases, the stress superposition increases gradually, forming a penetrating crack from the coal body to the rock mass. In addition, the mechanical model of coal-rock combined body is constructed, and the strength conditions of interface instability of coal-rock combined body are given.

DATA AVAILABILITY

All data used to support the findings of this study are included within the article, and there are not any restrictions on data access.

CONFLICTS OF INTEREST

The authors declare that they have no known competing financial interests or personal relationships that could have appeared to influence the work reported in this paper.

ACKNOWLEDGMENTS

The authors would like to thank the National Natural Science Foundation of China (No. 52304142, 52064042), Basic scientific research fees of colleges and universities directly under Inner Mongolia Autonomous Region (2023QNJS108), Program for Young Talents of Science and Technology in Universities of Inner Mongolia Autonomous Region (NJYT22073) and Natural Science Foundation of Inner Mongolia of China (2022MS05037) for supporting this work.

REFERENCES

Bai, J., Dou, L., Małkowski, P. et al.: 2021, Mechanical properties and damage behavior of rock-coal-rock combined samples under coupled static and dynamic loads. Geofluids, 3181697. DOI: 10.1155/2021/3181697

Chai, Y., Dou, L., Cai, W., et al.: 2023, Experimental investigation into damage and failure process of coal-rock composite structures with different roof lithologies under mining-induced stress loading. Int. J. Rock Mech. Min. Sci., 170, 105479. DOI: 10.1016/j.ijrmms.2023.105479

Chen, G.B., Li, T., Yang, L. et al.: 2021, Mechanical properties and failure mechanism of combined bodies with different coal-rock ratios and combinations. J. Min. Strata Control Eng., 3, 2, 84–94, (in Chinese). DOI: 10.13532/j.jmsce.cn10-1638/td.20210108.001

Chen, G.B., Li, T., Zhang, G.H. et al., 2023. Determination of bursting liability of coal-rock combined body based on residual energy release rate index. Chin. J. Rock Mech. Eng., 42, 6, 1366–1383, (in Chinese). DOI: 10.13722/j.cnki.jrme.2022.0882

Chen, G.B., Qin, Z.C., Zhang, G.H. et al.: 2020, Law of energy distribution before failure of loaded coal - rock combined body. Rock Soil Mech., 41, 6, 2021–2033, (in Chinese). DOI: 10.16285/j.rsm.2019.0101

Chen, G.B., Teng, P.C., Zhang, G.H. et al.: 2022, Fractal characteristics and energy transfer mechanism of coal-rock combined body fragments under different loading rates. Journal of Chongqing University, 45, 8, 115–129, (in Chinese). DOI: 10.11835/j.issn.1000-582X.2021.260

Chen, S.J., Li F.X., Yin D.W. et al.: 2023, Experimental study on deformation failure characteristics of limestone-coal composite with different rock-coal height ratios. J. Cent. South Univ. (Science and Technology), 54, 6, 2459–2472.
DOI: 10.11817/j.issn.1672-7207.2023.06.032

Cheng, Y.H., Jiang, F.X., Hu, Z.F. et al.: 2016, Prevention and control of coal burst on gob-side entry in deep coal seam with fully mechanized sublevel caving mining. Chin. J. Rock Mech. Eng., 35, S1, 3000–3007, (in Chinese). DOI: 10.13722/j.cnki.jrme.2014.1417

Feng, X.T., Xiao, Y.X., Feng, G.L. et al.: 2019, Study on the development process of rock bursts. Chin. J. Rock Mech. Eng., 38, 4, 649–673, (in Chinese). DOI: 10.13722/j.cnki.jrme.2019.0103

Gao, F.Q., Kang, H.P. and Yang, L.: 2020, Experimental and numerical investigations on the failure processes and mechanisms of composite coal-rock specimens. Sci. Rep., 1, 10, 13422.
DOI: 10.1038/s41598-020-70411-5

Gong, F.Q., Ye, H. and Luo, Y.: 2017, Rate effect on the burst tendency of coal-rock combined body under low loading rate range. J. China Coal Soc., 42, 11, 2852–2860, (in Chinese).
DOI: 10.13225/j.cnki.jccs.2017.0159

Shen, W.B., Yu, W.J. and Pan, B.: 2021, Rock mechanics test and failure characteristics of coal-rock combination with different dip angles. Miner. Eng. Res., 36, 1, 1–8, (in Chinese).
DOI: 10.13582/j.cnki.1674-5876.2021.01.001

Si, X.F., Luo, Y. and Luo, S.: 2024, Influence of lithology and bedding orientation on failure behavior of “D” shaped tunnel. Theor. Appl. Fract. Mech., 129, 104219. DOI: 10.1016/j.tafmec.2023.104219

Wang, X.N., Lu, C.P., Xue, J.H. et al.: 2013, Experimental research on rules of acoustic emission and microseismic effects of burst failure of compound coal-rock samples. Rock Soil Mech., 34, 9, 2569–2575, (in Chinese). DOI: 10.16285/j.rsm.2013.09.031

Yang, L., Gao, F.Q., Wang, X.Q. et al.: 2019, Energy evolution law and failure mechanism of coal-rock combined specimen. J. China Coal Soc., 44, 12, 3894–3902, (in Chinese).
DOI: 10.13225/j.cnki.jccs.2019.0011

Yang, K., Liu, W.J., Dou, L.T. et al.: 2020a, Experimental investigation into interface effect and progressive instability of coal-rock combined specimen. J. China Coal Soci. 45, 5, 1691–1700, (in Chinese).
DOI: 10.13225/j.cnki.jccs.DY20.0294

Yang, K., Liu, W.J., Ma, Y.K. et al.: 2022, Experimental study of impact failure characteristics of coal-rock combination bodies under true triaxial loading and single face unloading. Rock Soil Mech., 43, 1, 15–27, (in Chinese). DOI: 0.16285/j.rsm.2021.1101

Yang, L., Gao, F.Q. and Wang, X.Q.: 2020b, Mechanical response and energy partition evolution of coal-rock combinations with different strength ratios. Chin. J. Rock Mech. Eng., 39, 3297–3305, (in Chinese).
DOI: 10.13722/j.cnki.jrme.2020.0456

Yu, W.J., Wu, G.S., Liu, Z. et al.: 2020, Uniaxial compression test of coal-rock-bolt anchorage body and mechanical mechanisms of bolts. Chin. J. Rock Mech. Eng., 39, 1, 57–68, (in Chinese).
DOI: 10.13722/j.cnki.jrme.2019.0500

Yu, Y., Feng, X.T., Chen, B.R. et al.: 2013, Analysis of energy fractal and microseismic information characteristics about immediate rock bursts in deep tunnels with different excavation methods. Rock Soil Mech., 34, 9, 2622–2628, (in Chinese).
DOI: 10.16285/j.rsm.2013.09.040

Zhang, C.Y., Pan, J.F., Xia, Y.X. et al.: 2020, Research on impact failure characteristics of coal-rock combination bodies under true triaxial loading and unloading conditions. Chin. J. Rock Mech. Eng., 39, 8, 1522–1533, (in Chinese).
DOI: 10.13722/j.cnki.jrme.2020.0112

Zhang, X.Q., Wang, W.W., Jiang, Y.L., et al.: 2023, Mechanical properties and fracture damage law of coal-rock composition under the action of supercritical CO_2. J. China Coal Soc., 48, 11, 4049–4064, (in Chinese). DOI: 10.13225/j.cnki.jccs.2023.0118

Zhang, Z.T., Liu, J.F., Wang, L., et al.: 2012, Effects of combination mode on mechanical properties and failure characteristics of the coal-rock combinations. J. China Coal Soc., 37, 10, 1677–1681, (in Chinese).
DOI: 10.13225/j.cnki.jccs.2012.10.021

Zuo, J.P., Chen, Y. and Cui, F.: 2018, Investigation on mechanical properties and rock burst tendency of different coal-rock combined bodies. J. China Univ. Min. Technol., 47, 1, 81–87, (in Chinese).
DOI: 10.13247/j.cnki.jcumt.000795

Zuo, J.P., Xie, H.P., Meng, B.B., et al.: 2011, Experimental research on loading-unloading behavior of coal-rock combination bodies at different stress levels. Rock Soil Mech., 32, 5, 1287–1296, (in Chinese).
DOI: 10.16285/j.rsm.2011.05.028